MEMORANDUM REPORT BRL-MR-3803

BRL

OPTIMIZATION OF A PULSED AIR CORE TRANSFORMER FOR LOW IMPEDANCE INDUCTIVE IGNITION

ALEXANDER E. ZIELINSKI
JOHN A. BENNETT

JANUARY 1990

U.S. ARMY LABORATORY COMMAND

BALLISTIC RESEARCH LABORATORY
ABERDEEN PROVING GROUND, MARYLAND

DESTRUCTION NOTICE

Destroy this report when it is no longer needed. DO NOT return it to the originator.

Additional copies of this report may be obtained from the National Technical Information Service, U.S. Department of Commerce, Springfield, VA 22161.

The findings of this report are not to be construed as an official Department of the Army position, unless so designated by other authorized documents.

The use of trade names or manufacturers' names in this report does not constitute indorsement of any commerical product.

SECURITY CLASSIFICATION OF THIS PAGE

REPORT DOCUMENTATION PAGE

Form Approved
OMB No. 0704-0188

1a. REPORT SECURITY CLASSIFICATION UNCLASSIFIED	1b. RESTRICTIVE MARKINGS
2a. SECURITY CLASSIFICATION AUTHORITY	3. DISTRIBUTION / AVAILABILITY OF REPORT Approved for public release, Distribution unlimited.
2b. DECLASSIFICATION / DOWNGRADING SCHEDULE	
4. PERFORMING ORGANIZATION REPORT NUMBER(S) **BRL-MR-3803**	5. MONITORING ORGANIZATION REPORT NUMBER(S)
6a. NAME OF PERFORMING ORGANIZATION U.S. Army Ballistic Research Laboratory 6b. OFFICE SYMBOL (If applicable) SLCBR-TB-EP	7a. NAME OF MONITORING ORGANIZATION
6c. ADDRESS (City, State, and ZIP Code) Aberdeen Proving Ground, MD 21005-5066	7b. ADDRESS (City, State, and ZIP Code)
8a. NAME OF FUNDING / SPONSORING ORGANIZATION AMCCOM, JSSAP, Close Combat Armaments Center 8b. OFFICE SYMBOL (If applicable) SMCAR-CCL-FA	9. PROCUREMENT INSTRUMENT IDENTIFICATION NUMBER
8c. ADDRESS (City, State, and ZIP Code) Picatinny Arsenal, Dover, NJ 07801-5001	10. SOURCE OF FUNDING NUMBERS PROGRAM ELEMENT NO. 6122IA; PROJECT NO. AH21; TASK NO. 00; WORK UNIT ACCESSION NO. 001AJ

11. TITLE (Include Security Classification)
Optimization of a Pulsed Air Core Transformer for Low Impedance Inductive Ignition
Unclassified

12. PERSONAL AUTHOR(S)
Alexander E. Zielinski (BRL) and John A. Bennett (ARDEC)

13a. TYPE OF REPORT	13b. TIME COVERED	14. DATE OF REPORT (Year, Month, Day)	15. PAGE COUNT
MR	FROM _____ TO _____		

16. SUPPLEMENTARY NOTATION
This work was performed while the authors were located at Picatinny Arsenal, ARDEC, Dover, NJ.

17. COSATI CODES			18. SUBJECT TERMS (Continue on reverse if necessary and identify by block number)
FIELD	GROUP	SUB-GROUP	PULSE TRANSFORMER
10	01		IGNITION
21	03		PULSED POWER

19. ABSTRACT (Continue on reverse if necessary and identify by block number)
A design analysis was conducted to develop an inductive ignition concept for ordnance. Mathematical models were developed to examine the transformer for optimum performance. Results indicate that significant energy transfer to an electric primer can be obtained using a simple pulse transformer. Experimental results using a capacitive pulsed power supply indicate reasonable agreement with the models for short times. Deviations from the theoretical model can be explained by nonlinear materials effects and field diffusion in the surrounding barrel walls.

20. DISTRIBUTION / AVAILABILITY OF ABSTRACT	21. ABSTRACT SECURITY CLASSIFICATION
X ☐ UNCLASSIFIED/UNLIMITED ☐ SAME AS RPT ☐ DTIC USERS	UNCLASSIFIED

22a. NAME OF RESPONSIBLE INDIVIDUAL	22b. TELEPHONE (Include Area Code)	22c. OFFICE SYMBOL
Alex Zielinski	(303) 278-3889	SLCBR-TB-EP

DD Form 1473, JUN 86 *Previous editions are obsolete*

SECURITY CLASSIFICATION OF THIS PAGE

INTENTIONALLY LEFT BLANK.

Table of Contents

INTENTIONALLY LEFT BLANK.

List of Figures

INTENTIONALLY LEFT BLANK.

ACKNOWLEDGEMENTS

The assistance of Dr. John Powell and Mr. Henry Burden of the Ballistics Research Laboratory is gratefully acknowledged in the preparation of this manuscript.

INTENTIONALLY LEFT BLANK.

I. INTRODUCTION

Alternative approaches to gun propellant ignition have been explored to ease automatic handling and loading of large caliber ammunition. Automatic loading is facilitated by incorporating a sliding block breech mechanism. Advantages obtained by eliminating a separately loaded primer for the ammunition include advanced rapid fire artillery systems, integrated system simplification, and, increased reliability and safety. A further advantage is the lower strength requirement on the propellant case due to the absense of a percussion pin.

This investigation addresses a low impedance inductive ignition (LI^3) concept design using a simple pulsed air-core transformer to transfer energy to an electrically initiated primer embedded in an igniter pad at the base of the propelling charge. The transformer consists of a single turn copper primary coil in the breech face and a consumable lead secondary in the charge as shown in Figure 1. Because of the transformer's topology, conventional percussive primer ignition systems can still be used. Low transformer efficiency coupled with high capacitive energy densities makes this an attractively insensative ignition scheme.

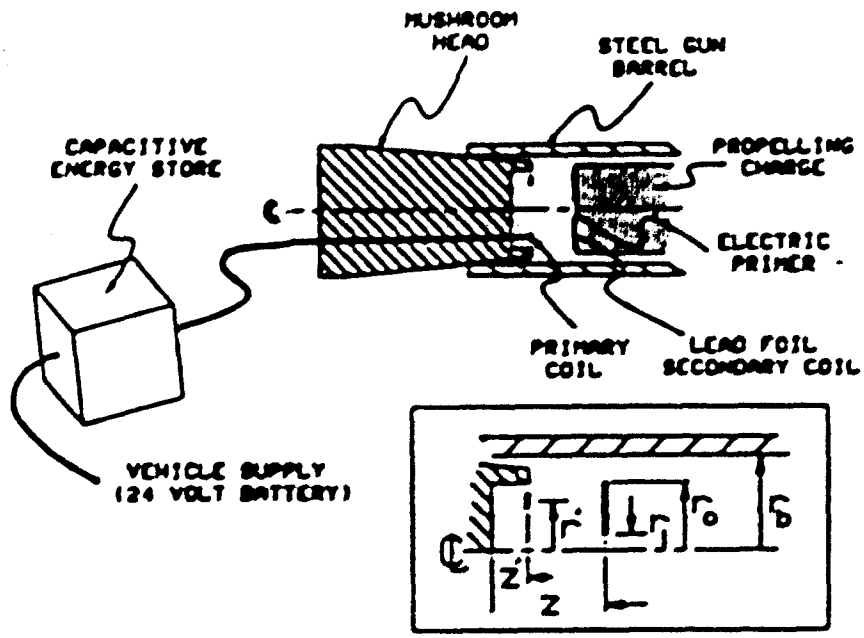

Figure 1. LI^3 concept.

Previous work [1] on the LI^3 ignition system examined the capacitive energy store, charging circuit, and electric primer requirements using a lumped parameter electric circuit model. To improve performance, it was desirable to configure the circuitry for the fastest possible pulse. The coupling between coils and barrel, a complex function of geometry, substantially determines transformer performance, and was modeled using a single, average mutual inductance obtained from various experimental data. This paper describes an analysis of the magnetic fields of the pulse transformer directed towards an accurate

prediction of primary/secondary coil coupling and optimum performance.

II. ANALYTICAL MODEL

The electromagnetic field analysis of the transformer requires a mathematical derivation of the vector potential inside the combustion chamber and subsequent computation to determine transformer geometry for optimum energy transfer to the electric primer load. The impedance of the charging circuit is considered dominant, resulting in the primary current pulse profile being nearly independent of the transformer geometry. The duration of this event is on the order of tens of microseconds; consequently, the magnetic flux is substantially excluded from the interior of the conductors. In addition, the primary coil is taken to be filamentary, minimizing the reluctance inside the chamber.

The vector potential, A, inside the combustion chamber is the solution to Poisson's equation in cylindrical coordinates. The magnitude of the azimuthal component is expressed as follows

$$\frac{\partial^2 A}{\partial r^2} + \frac{1}{r}\frac{\partial A}{\partial r} + \frac{\partial^2 A}{\partial z^2} - \frac{A}{r^2} = -\mu J \tag{1}$$

where A vanishes on the surface of the chamber. The permeability is μ and J is the primary coil current density. The secondary coil is a very thin foil, and its contribution to the vector potential is considered negligible. Equation 1 is solved with a Green's function, $G(r, \dot{r})$, constructed from the electrostatic potential of a point charge at $\dot{r}$, $\dot{\phi}$, and $\dot{z}$, inside a conducting cylinder comprising surfaces $r = r_b$ and $z = 0$ at zero potential [2]

$$G(r,\dot{r}) = \frac{1}{2\pi r_b^2}\sum_{n=1}^{\infty}\sum_{m=0}^{\infty}(2-\delta_m^o)[e^{(-x_n|z-\dot{z}|)} - e^{(-x_n|z+\dot{z}|)}]\left[\frac{J_m(x_n\dot{r})J_m(x_n r)}{x_n[J_{m+1}(x_n r_b)]^2}\right]\cos(m(\phi-\dot{\phi})) \tag{2}$$

where J_m and J_{m+1} are Bessel functions, x_n is defined by $J_1(x_n r_b) = 0$, and δ_m^o is the Kronecker delta. The solution to the Poisson equation (1) is given by

$$A = \mu I_1 \oint_\ell G(r,\dot{r})\,\dot{r}\,\cos(\phi-\dot{\phi})\,d\dot{\phi} \tag{3}$$

where I_1 is the primary current. Substituting the Green's function (2) into equation (3) and performing the integration yields

$$A = \mu I_1\left(\frac{\dot{r}}{r_b^2}\right)\sum_{n=1}^{\infty}[e^{(-x_n|z-\dot{z}|)} - e^{(-x_n|z+\dot{z}|)}]\left[\frac{J_1(x_n\dot{r})J_1(x_n r)}{x_n[J_2(x_n r_b)]^2}\right] \tag{4}$$

where $\acute{r}$, $\acute{z}$ are the cylindrical coordinates of the primary coil and r_b is the radius of the combustion chamber. The current in the secondary coil, I_2, may be calculated from Faraday's law

$$\dot{\phi} + \frac{2\pi r J_{sec}}{\sigma} + I_2 R_{load} = 0 \tag{5}$$

where σ is the conductivity of the secondary coil, J_{sec} is the secondary current density, and R_{load} is the resistance of the electric primer.

Substitution of $2\pi\, r\dot{A} = \dot{\phi}$ and subsequent integration in terms of thickness δ, and inner and outer radii r_i and r_o of the secondary coil yields the transfer function [3]

$$\alpha = \mu \left(\frac{\acute{r}}{r_b^2}\right) \left[\frac{1}{\sigma\delta} + \frac{R_{load}}{2\pi} \ln(r_o/r_i)\right]^{-1} \sum_{n=1}^{\infty} [e^{(-x_n|z-\acute{z}|)} - e^{(-x_n|z+\acute{z}|)}] \left[\frac{J_1(x_n\acute{r})[J_0(x_n r_o) - J_0(x_n r_i)]}{x_n^2[J_2(x_n r_b)]^2}\right] \tag{6}$$

where α is the ratio $I_2/\dot{I}_1$.

The transfer function equation (6) is evaluated for a 155 mm Self Propelled Howitzer with a combustion chamber radius, r_b, equal to 60.3 mm. On the basis of materials considerations, performance criteria, and breech design constraints, a primary coil of 12 gage square magnet wire is selected and mounted in a 12.7 mm recessed section. The mean axial location of the primary coil from the breech is 11.7 mm. The secondary coil is made from 0.1 mm thick lead (Pb) foil and its axial position from the breech is denoted by z. All radial dimensions for the coil geometries are normalized to the combustion chamber radius. A numerical technique was implemented to find the optimum primary coil mean radius and the secondary coil inner and outer radii when the transfer function is maximized. The primary/secondary coil separation distance is defined by

$$z_{1,2} = z - \acute{z}. \tag{7}$$

The optimum value for α at a separation distance of 2 mm is 3.480×10^{-7} seconds. Using the optimized coil dimensions for 200 mm of separation, and calculating α at 2 mm gives 2.837×10^{-7} seconds, only 18.6% less. This deviation from optimum quickly falls below 5% for $z_{1,2}$ greater than 12.7 mm and indicates the insensitivity of the transfer function to radially varying coil dimensions. For the three coil parameters, $\acute{r}$, r_i, and r_o, the optimum coil dimension variation as a function of primary/secondary separation is plotted in Figure 2. In addition, transformer performance degrades with increasing primary/secondary separation distance as illustrated in Figure 3.

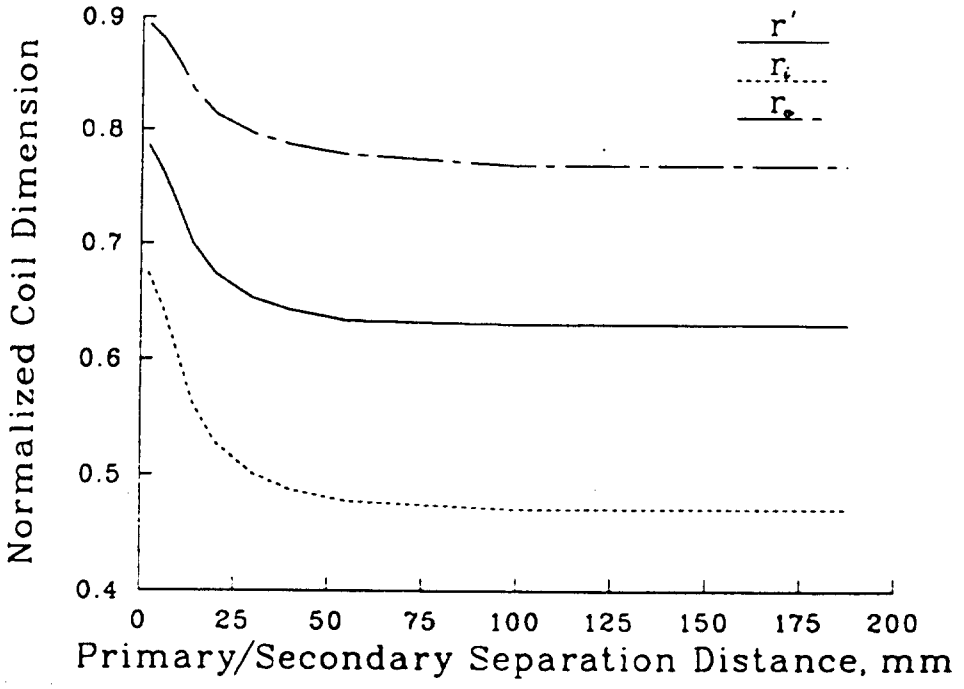

Figure 2. Coil dimensions normalized to r_b versus separation distance.

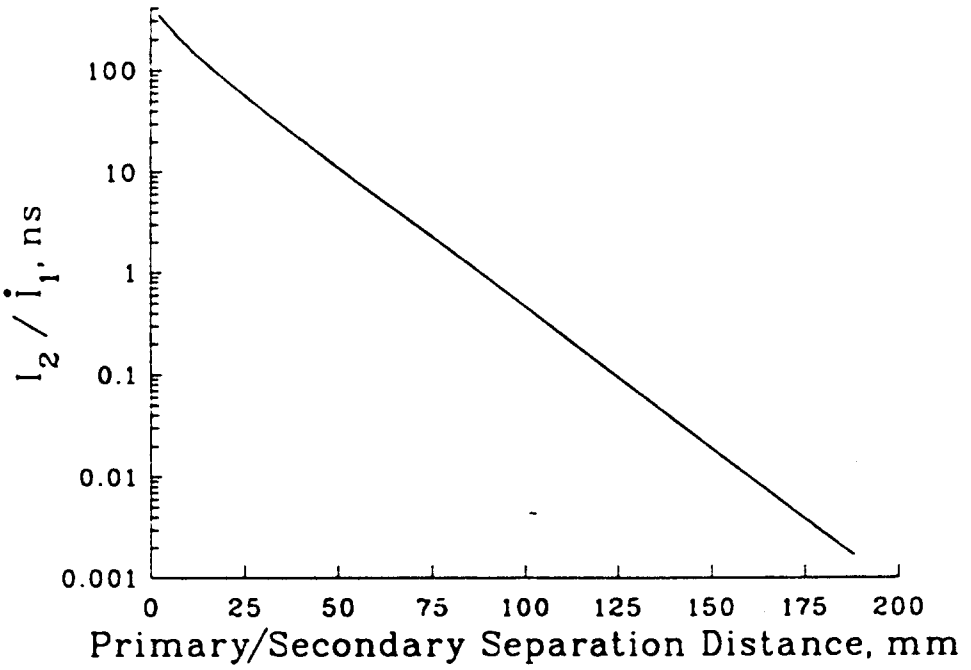

Figure 3. Transfer function versus separation distance.

Relaxation of design restrictions on the secondary circuit impacts system effectiveness. Optimum values for the transfer function were calculated with $z_{1,2}$ fixed at 100 mm. Results from varying the foil thickness and electric primer load resistance are illustrated in Figure 4. Thicker secondary coils have reduced ohmic losses but may leave large amounts of residue in the barrel. In all cases, lower electric primer resistance yields a larger value for the transfer function. The optimum, normalized, primary coil radius for this variational analysis remained constant at 0.63. However, the secondary foil width ($r_o - r_i$) decreased with an increasing mean secondary radius for thicker foils.

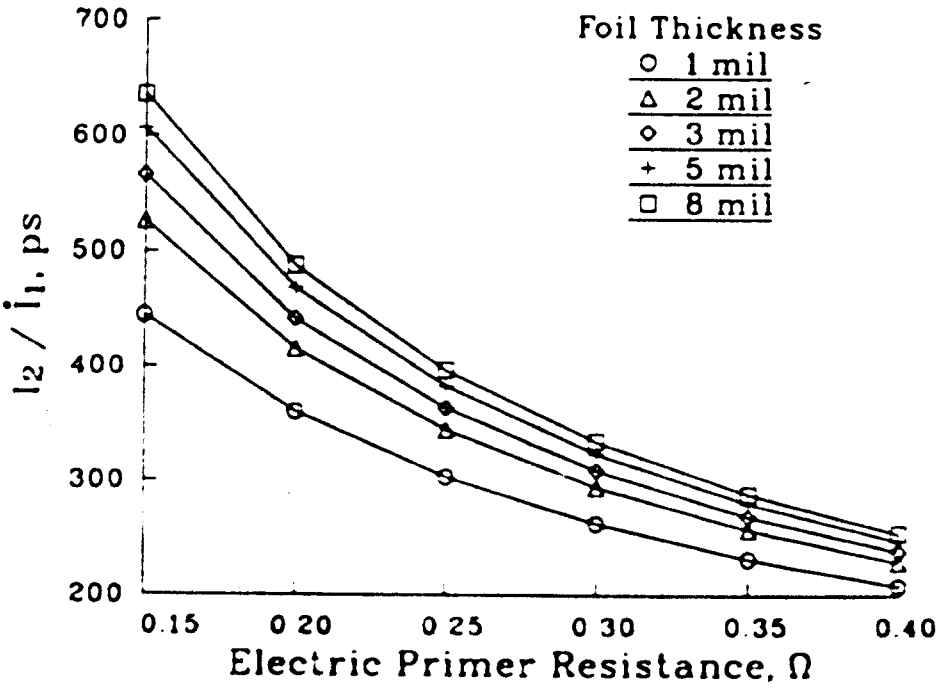

Figure 4. Transfer function versus electric primer resistance.

III. EXPERIMENTAL RESULTS AND DISCUSSION

The experiments were performed using a conventional 155 mm breech with a 12 gage square copper coil having a mean radius of 39 mm embedded in the breech face. The mushroom head recess diameter was 121 mm; the steel gun barrel which fit over the spindle had an inner diameter of 142 mm. The gun barrel radius was used for r_b in normalizing all coil configuration dimensions. The power supply specifications were developed at ARDEC and built by EML, Inc. It stores nominally 1500 Joules at 5 kV. All secondary test coils used 0.13 mm thick copper foil with a 0.174 Ω load resistor. The resulting normalized primary coil radius is 0.55 and the normalized secondary coil dimension domain is bounded by $0.36 < r_i < 0.76$, and $0.56 < r_o < 0.94$. Data on each coil configuration, identified by H, D, C, and K, are given later in Table 1.

Earlier circuit analysis had indicated that increased performance would be obtained

by minimizing the primary side inductance and resistance.[1] The transmission line leads from the power supply to the breech were fabricated from high voltage coax with a length of 2.7 m. A ringing pulse discharge with the primary coil connected yielded 2.5μH and 28.6$m\Omega$ for the primary side circuit parameters. During each test, initial charge voltage, primary current, and secondary load voltage were recorded. The current was measured using a current transformer while the secondary voltage was measured directly with a voltage divider. Figure 5 shows a typical trace obtained for the measured primary current and secondary load voltage at an initial charge voltage of 1 kV. Also shown is the primary di/dt, obtained by differentiating the primary current. Differentiation is done via a numerical technique which uses a five point smoothing algorithm. During all tests the primary to secondary distance remained constant at 44.13 mm.

Twenty four tests were performed with each of the four coil configurations pulsed twice at initial charge voltages of 1, 3, and 5 kV. For each test α could be found as a function of time from

$$\alpha(t) = \frac{I_2(t)}{\dot{I}_1(t)} = \frac{V_2(t)/0.174\Omega}{\Delta I_1(t)/\Delta t}. \tag{8}$$

Typical waveforms obtained using equation (8) are shown in Figure 6 for the four coil configurations at an initial charge voltage of 3 kV. For times greater than 7μs there is very little deviation amongst the four coils. Beyond 16μs the value of $I_2/\dot{I}_1$ becomes untenably large as $\dot{I}_1$ approaches zero.

For all coil configurations, the transfer function data are only significantly different for times less than 5 μsec. The time averaged values of α, integrated over the interval .5 μsec to 22 μsec, for all coil configurations is 51.44×10^{-9} seconds with a deviation of only 2.8%. Since the mathematical model is applicable only when the vector potential on the inner barrel wall surface is zero, the data should be evaluated for short times. A time of 3 μsec was selected to analyze $I_2/\dot{I}_1$. The deviation of the transfer function among the four coil configurations evaluated at this time is 16.8%. Table 1 lists α for the four coil configurations tested in order of decreasing $I_2/\dot{I}_1$. Also, results from the theoretical model are shown to be in reasonable agreement with the experimental data.

Table 1. Coil Configuration Summary

Coil Configuration	r_i	r_o	$I_2/\dot{I}_1$, 10^{-9} seconds	
			Data @ 3μs	Calculated
H	.36	.56	30.71 ± 3.0%	28
D	.51	.87	27.37 ± 9.3%	32
C	.60	.78	24.86 ± 6.4%	34
K	.76	.94	20.38 ± 10.4%	21

The weak dependence of α on secondary radial coil dimensions for the domain $r_i < 0.6$, and $r_o > 0.6$, is illustrated for the laboratory setup ($\dot{r} = 0.55$) in Figure 7. The optimum

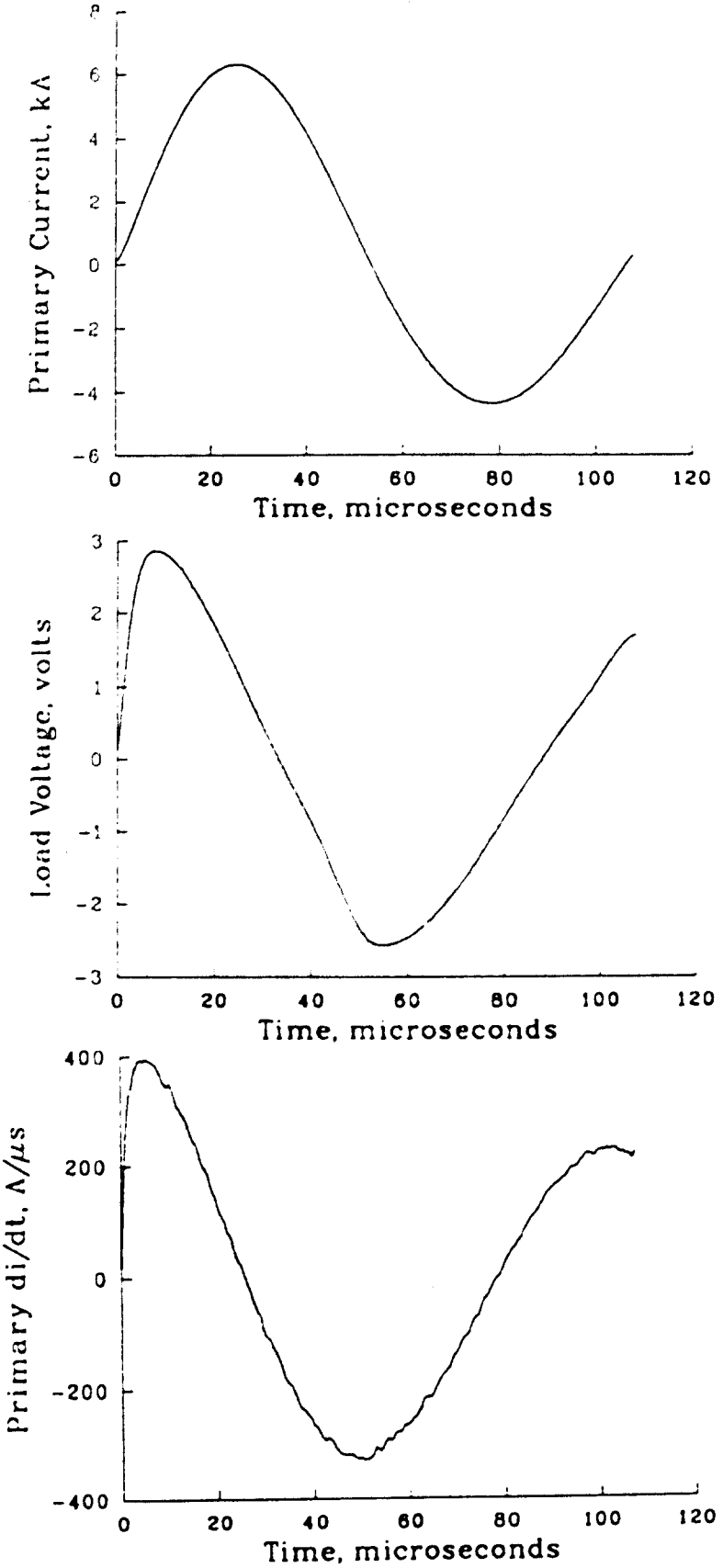

Figure 5. Measured primary coil current (top) and secondary load voltage (middle) and differentiated primary coil current (I_1, bottom).

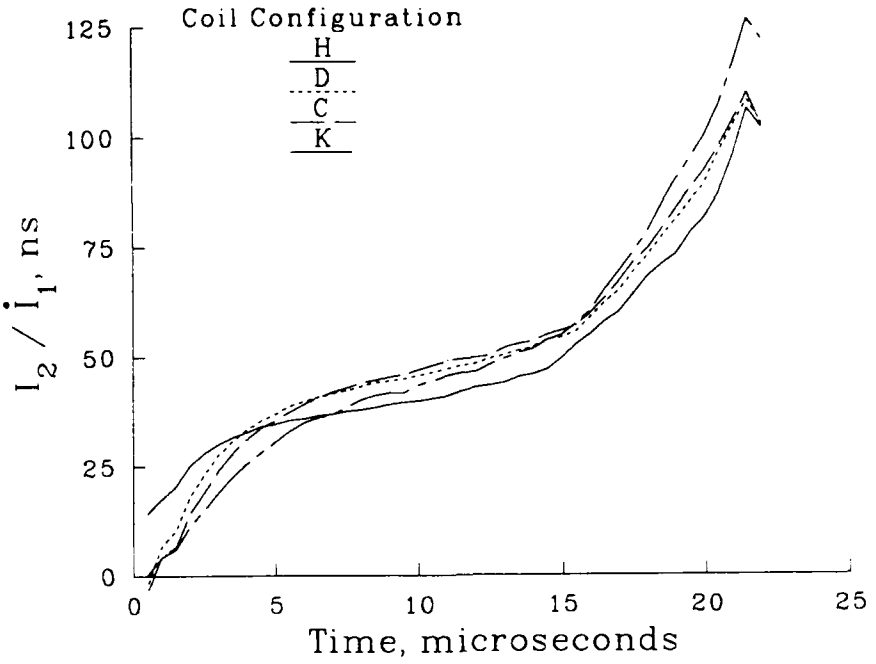

Figure 6. Transfer functions for coils H, D, C, and K.

normalized secondary coil dimensions are $r_i = 0.56$ and $r_o = 0.69$. The corresponding calculated transfer function is 35×10^{-9} seconds; this is a 14 % increase over the largest measured, and is near the uncertainty in the experimental data.

The value of $I_2/\dot{I}_1$ varied as much as 10.4% as the capacitor bank voltage was increased. Nonlinear effects arising from the presence of the steel barrel containment become apparent when considering the energy transferred to the secondary load. Therefore, the efficiency, η, defined as the ratio of the secondary load energy to the stored capacitive energy, is given as

$$\eta = \frac{\int \frac{V_2(t)^2}{R_{load}} dt}{E_{stored}}. \tag{9}$$

For all test voltages configuration C was found to transfer energy most efficiently while coil configuration H was found least efficient. Efficiency was found to decrease as the capacitor voltage was increased. The variation of magnetic permeability with magnetic flux density at the surrounding barrel wall alters the induced ohmic losses. The effect is illustrated in Figure 8. As would be expected, relatively more energy was transferred to the 0.174 Ω load at the higher voltages.

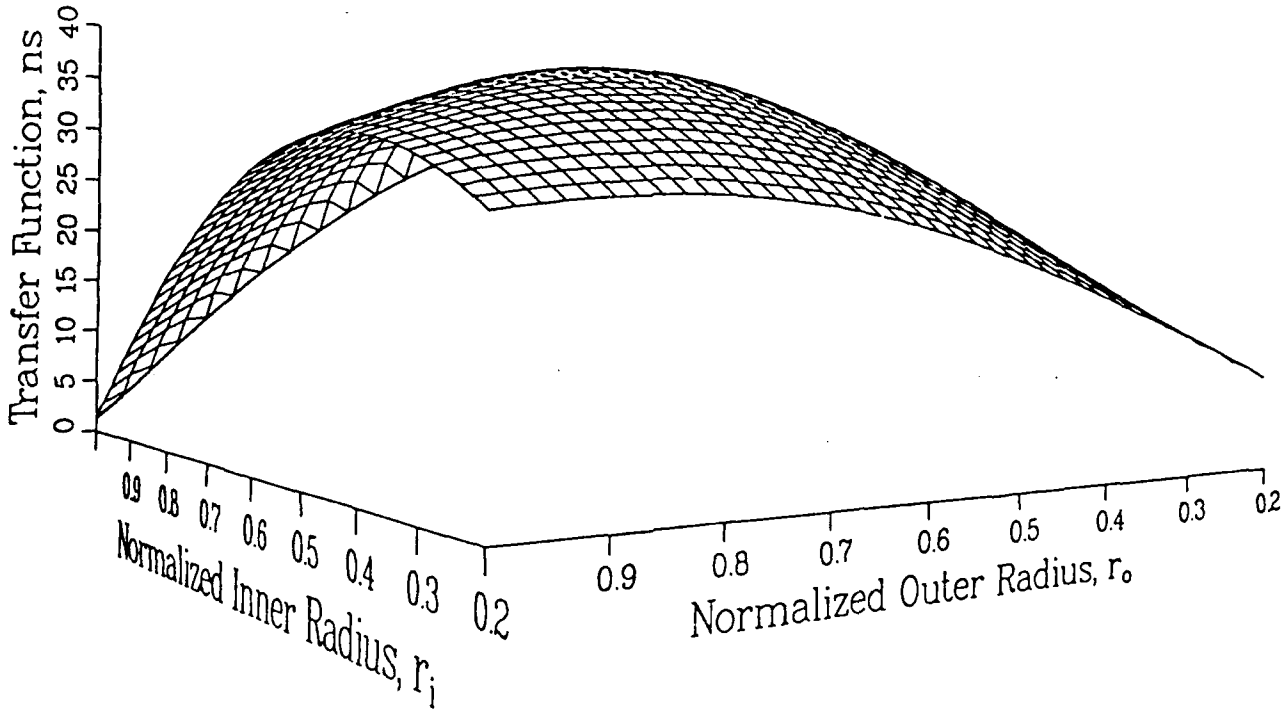

Figure 7. Transfer function surface corresponding to the laboratory setup ($\acute{r} = 0.55$) plotted as a function of secondary radii.

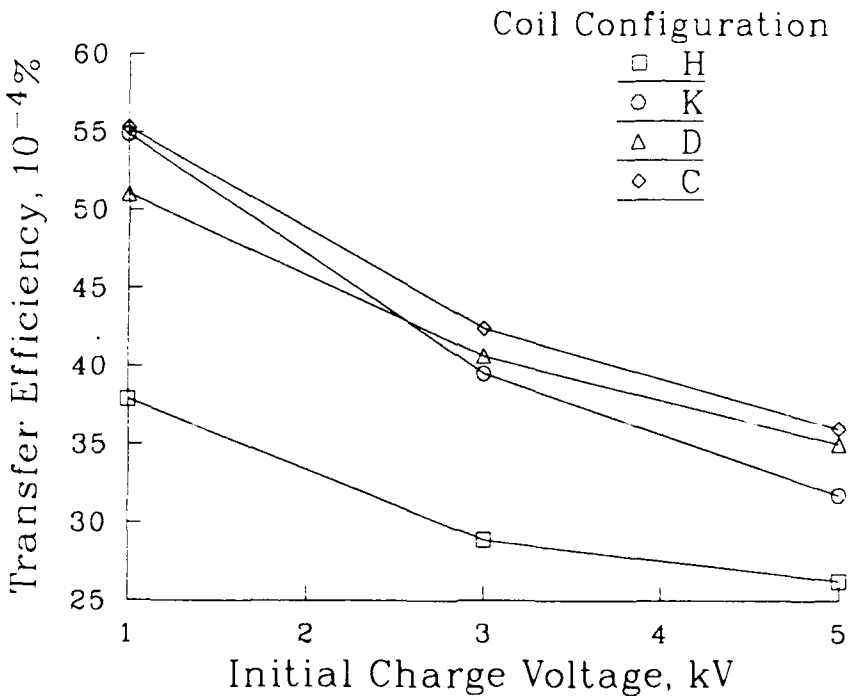

Figure 8. Transfer efficiency versus initial capacitor voltage.

IV. CONCLUSIONS

Corresponding to the optimum performance configuration, the primary coil mean radius and the secondary coil inner and outer radii attain nearly constant values with increasing primary/secondary coil separation distance. The transfer function was found to be relatively insensitive to small changes in coil radial dimensions near optimum. The theoretical model assumed simple dimensional boundaries while the experiment used actual gun barrel hardware which produced small dimensional deviations from the assumed model. These too were found to offer undiscernible differences between tranfer function calculations and experimental data. Pulse times greater than $7\mu s$ produced little variation in the transfer function among the tested coil configurations. Limiting the diffusion of the magnetic flux in the surrounding barrel steel with a fast discharge pulse should lead to the conditions assumed in the transformer model and optimum transformer performance. Inclusion of the permeable, surrounding barrel material in the analysis will require further work. Additional experimental work is needed in order to verify the theoretical model presented. Better selection of coil configurations is needed to explore the theoretical model in the domains $r_i > 0.4$, $r_o < 0.6$ and $r_i > 0.6$, $r_o > 0.9$, where the change in α is most sensitive to the change in coil dimensions.

These results are intended to support a refined system design for further experimental verification of the low impedance inductive ignition concept.

References

1. Bennett, John and Zielinski, Alex, "Low Impedance Inductive Ignition," Journal of Ballistics, vol 8, issue 3, 1984.

2. Smythe, William R., "Static and Dynamic Electricity," Second Edition, McGraw-Hill Book Company, Inc., 1950.

3. Abramowitz, M. and Stegun, I.,"Handbook of Mathematical Functions," Dover Publishing, Inc., 1972.

INTENTIONALLY LEFT BLANK.

No of Copies	Organization
(Unclass., unlimited) 12	Administrator
(Unclass., limited) 2	Defense Technical Info Center
(Classified) 2	ATTN: DTIC-DDA
	Cameron Station
	Alexandria, VA 22304-6145
1	HQDA (SARD-TR)
	WASH DC 20310-0001
1	Commander
	US Army Materiel Command
	ATTN: AMCDRA-ST
	5001 Eisenhower Avenue
	Alexandria, VA 22333-0001
1	Commander
	US Army Laboratory Command
	ATTN: AMSLC-DL
	Adelphi, MD 20783-1145
2	Commander
	Armament RD&E Center
	US Army AMCCOM
	ATTN: SMCAR-MSI
	Picatinny Arsenal, NJ 07806-5000
2	Commander
	Armament RD&E Center
	US Army AMCCOM
	ATTN: SMCAR-TDC
	Picatinny Arsenal, NJ 07806-5000
1	Director
	Benet Weapons Laboratory
	Armament RD&E Center
	US Army AMCCOM
	ATTN: SMCAR-LCB-TL
	Watervliet, NY 12189-4050
1	Commander
	US Army Armament, Munitions
	and Chemical Command
	ATTN: SMCAR-ESP-L
	Rock Island, IL 61299-5000
1	Commander
	US Army Aviation Systems Command
	ATTN: AMSAV-DACL
	4300 Goodfellow Blvd.
	St. Louis, MO 63120-1798
1	Director
	US Army Aviation Research
	and Technology Activity
	Ames Research Center
	Moffett Field, CA 94035-1099

No of Copies	Organization
1	Commander
	US Army Missile Command
	ATTN: AMSMI-RD-CS-R (DOC)
	Redstone Arsenal, AL 35898-5010
1	Commander
	US Army Tank Automotive Command
	ATTN: AMSTA-TSL (Technical Library)
	Warren, MI 48397-5000
1	Director
	US Army TRADOC Analysis Command
	ATTN: ATAA-SL
	White Sands Missile Range, NM 88002-5502
(Class. only) 1	Commandant
	US Army Infantry School
	ATTN: ATSH-CD (Security Mgr.)
	Fort Benning, GA 31905-5660
(Unclass. only) 1	Commandant
	US Army Infantry School
	ATTN: ATSH-CD-CSO-OR
	Fort Benning, GA 31905-5660
(Class. only) 1	The Rand Corporation
	P.O. Box 2138
	Santa Monica, CA 90401-2138
1	Air Force Armament Laboratory
	ATTN: AFATL/DLODL
	Eglin AFB, FL 32542-5000

Aberdeen Proving Ground

Dir, USAMSAA
ATTN: AMXSY-D
AMXSY-MP, H. Cohen

Cdr, USATECOM
ATTN: AMSTE-TO-F

Cdr, CRDEC, AMCCOM
ATTN: SMCCR-RSP-A
SMCCR-MU
SMCCR-MSI

Dir, VLAMO
ATTN: AMSLC-VL-D

No. of Copies	Organization
5	Commander Armament RD&E Center US Army AMCCOM ATTN: SMCAR-FSE (Dr. T. Gora, John Bennett) SMCAR-AEE-B (Dr. D. Downs) SMCAR-CCL-FA (H. Moore, H. Kahn) Picatinny Arsenal, NJ 07806-5000
2	Director Benet Weapons Laboratory Armament RD&E Center US Army AMCCOM ATTN: SMCAR-LCB-DS (Dr. C. A. Andrade) SMCAR-CCB-RM (Dr. Pat Vottis) Watervliet, NY 12189
1	Director DARPA ATTN: Dr. Peter Kemmey 1400 Wilson Blvd. Arlington, VA 22209
1	Commander SDIO ATTN: SDIO/IST (MAJ M. Huebschman) Washington, DC 20301-7100
1	CG, MCRDAC Code AWT ATTN: Carroll Childers Quantico, VA 22134-5080
1	Director US Army Research Office ATTN: Dr. Michael Ciftan P. O. Box 12211 Research Triangle Park, NC 27709-2211
2	Air Force Armament Laboratory ATTN: AFATL/DLJG (Mr. Kenneth Cobb) AFATL/DLDG (Dr. T. Aden) Eglin AFB, FL 32542-5000
1	Director Brookhaven National Laboratory ATTN: Dr. J. R. Powell Bldg 129 Upton, NY 11973

No. of Copies	Organization
1	Director Lawrence Livermore National Laboratory ATTN: Dr. R. S. Hawke, L-156 P. O. Box 808 Livermore, CA 94550
3	Director Los Alamos National Laboratory ATTN: MSG 787, Mr. Max Fowler Dr. J. V. Parker Dr. William Condit Los Alamos, NM 87545
1	Sandia National Laboratory ATTN: Dr. Maynard Cowan Dept. 1220 P. O. Box 5800 Albuquerque, NM 87185
1	NASA Lewis Research Center ATTN: MS 501-7 (Lynette Zana) 2100 Brook Park Road Cleveland, OH 44135
1	Astron Research & Engineering ATTN: Dr. Charles Powars 130 Kifer Court Sunnyvale, CA 94086
2	Austin Research Associates ATTN: Dr. Millard L. Sloan Dr. William E. Drummond 1091 Rutland Drive Austin, TX 87858
3	Maxwell Laboratories ATTN: Dr. Rolf Dethlefson Dr. Michael M. Holland Dr. Mark Wilkinson 8888 Balboa Avenue San Diego, CA 92123
1	Boeing Aerospace Company ATTN: Dr. J. E. Shrader P. O. Box 3999 Seattle, WA 98134
2	GA Technologies, Inc. ATTN: Dr. Robert Bourque Dr. L. Holland P. O. Box 85608 San Diego, CA 92138

No. of Copies	Organization
2	GT Devices ATTN: Dr. Shyke Goldstein Dr. D. Tidman 5705-A General Washington Drive Alexandria, VA 22312
1	General Dynamics ATTN: Dr. Jaime Cuadros P. O. Box 2507 Pomona, CA 91766
2	Electromagnetic Research, Inc. ATTN: Dr. Henry Kolm Dr. Peter Mongeau 2 Fox Road Hudson, MA 01749
2	General Electric Company (AEPD) ATTN: Dr. William Bird Dr. Slade L. Carr R. D. #3, Plains Road Ballston Spa, NY 12020
1	General Research Corporation ATTN: Dr. William Isbell 5383 Hollister Avenue Santa Barbara, CA 93111
2	IAP Research, Inc. ATTN: Dr. John P. Barber Mr. David P. Bauer 2763 Culver Avenue Dayton, OH 45429-3723
2	LTV Aerospace & Defense Company ATTN: MS TH-83, Dr. Michael M. Tower Dr. C. H. Haight P. O. Box 650003 Dallas, TX 75265-0003
1	Pacific-Sierra Research Corp. ATTN: Dr. Gene E. McClellan 1401 Wilson Blvd. Arlington, VA 22209
2	Physics International Company ATTN: Dr. A. L. Brooks Dr. Frank Davies 2700 Merced Street San Leandro, CA 945771
1	R&D Associates ATTN: Dr. Peter Turchi P. O. Box 9695 Marina del Rey, CA 90291
3	SAIC ATTN: Dr. Jad H. Batteh Dr. G. Rolader Mr. L. Thornhill 1503 Johnson Ferry Rd., Suite 100 Marietta, GA 30062
1	System Planning Corporation ATTN: Donald E. Shaw 1500 Wilson Blvd. Arlington, VA 22209
2	Westinghouse Electric Corporation Marine Division ATTN: Dr. Dan Omry Dr. Ian R. McNab 401 East Hendy Avenue Sunnyvale, CA 94088-3499
1	Westinghouse R&D Laboratory ATTN: Dr. Bruce Swanson 1310 Beulah Road Pittsburgh, PA 15233
2	Auburn University ATTN: Dr. Raymond F. Askew Leach Nuclear Science Center Dr. E. J. Clothiaux Department of Physics Auburn University, AL 36849-3501
1	Texas Technical University Department of EE/Computer Science ATTN: Dr. M. Kristiansen Lubbock, TX 79409-4439
1	Tuskegee Institute Dept. of Mechanical Engineering ATTN: Dr. Pradosh Ray Tuskegee Institute, AL 36088
1	University of Alabama in Huntsville School of Science & Engineering ATTN: Dr. C. H. Chen Huntsville, AL 35899
1	University of Miami ATTN: Dr. Manuel A. Huerta, Physics Dept. P.O. Box 248046 Coral Gables, FL 33124

No. of Copies	Organization
1	University of Tennessee Space Institute ATTN: Dr. Dennis Keefer Tullahoma, TN 37388-8897
3	University of Texas Center for Electromechanics Balcones Research Center ATTN: Mr. William Weldon Mr. Raymond Zaworka Dr. Harry Fair 10100 Burnet Road, Bldg. 133 Austin, TX 78748
1	Dr. E. W. Sucov 1065 Lyndhurst Drive Pittsburgh, PA 15206
1	SAIC, Inc. ATTN: Dr. K. A. Jamison 1247-B North Eglin Parkway Shalimar, FL 32579
	Aberdeen Proving Ground
1	Cdr, USATECOM ATTN: AMSTE-SI-F

USER EVALUATION SHEET/CHANGE OF ADDRESS

This Laboratory undertakes a continuing effort to improve the quality of the reports it publishes. Your comments/answers to the items/questions below will aid us in our efforts.

1. BRL Report Number MR-3803 Date of Report JAN 90

2. Date Report Received _____

3. Does this report satisfy a need? (Comment on purpose, related project, or other area of interest for which the report will be used.) _____

4. How specifically, is the report being used? (Information source, design data, procedure, source of ideas, etc.) _____

5. Has the information in this report led to any quantitative savings as far as man-hours or dollars saved, operating costs avoided or efficiencies achieved, etc? If so, please elaborate. _____

6. General *Comments*. *What* do you think should be changed to improve future reports? (Indicate changes to organization, technical content, format, etc.)

_____

_____

_____

CURRENT ADDRESS

_____
Name

_____
Organization

_____
Address

_____
City, State, Zip

7. If indicating a Change of Address or Address Correction, please provide the New or Correct Address in Block 6 above and the Old or Incorrect address below.

OLD ADDRESS

_____
Name

_____
Organization

_____
Address

_____
City, State, Zip

(Remove this sheet, fold as indicated, staple or tape closed, and mail.)

FOLD HERE

Director
U.S. Army Ballistic Research Laboratory
ATTN: SLCBR-DD-T
Aberdeen Proving Ground, MD 21005-5066

NO POSTAGE
NECESSARY
IF MAILED
IN THE
UNITED STATES

OFFICIAL BUSINESS

BUSINESS REPLY MAIL
FIRST CLASS PERMIT NO 12062 WASHINGTON, DC

POSTAGE WILL BE PAID BY DEPARTMENT OF THE ARMY

Director
U.S. Army Ballistic Research Laboratory
ATTN: SLCBR-DD-T
Aberdeen Proving Ground, MD 21005-9989

FOLD HERE